Sensors and Materials, Vol. 16, No. 1 (2004) 159–169
MYU Tokyo

S & M 0554

Surface Micromachined Pressure Sensing Structures with Biocompatible Interface

Ebin Liao*, Simon Ang, Andrew Tay Ah Ong,
Yung C. Liang[1] and Adrian Yap U. Jin[2]

Department of Mechanical Engineering, National University of Singapore,
10 Kent Ridge Crescent, Singapore 119260
[1]Department of Electrical and Computer Engineering, National University of Singapore,
10 Kent Ridge Crescent, Singapore 119260
[2]Department of Restorative Dentistry, National University of Singapore,
5 Lower Kent Ridge Road, Singapore 119074

(Received December 18, 2003; accepted May 13, 2004)

Key words: temporomandibular disorder, surface micromachining, pressure sensor, biocompatible interface

Surface micromachined poly-Si pressure-sensing structures with biocompatible interfaces were developed for therapy of temporomandibular disorder (TMD). These structures made use of poly-Si suspended bridges, modified bridges with etching holes, and crossing bridges as flexible capacitor plates. Two biocompatible materials were considered as the interfaces between the pressure-sensing structures and the tooth. Optimization and testing were conducted on different sensor schemes, and the measurements were compared with the simulation results. Compared with conventional methods, this microsensor enables the continuous monitoring of the grinding activities of TMD patients and is less injurious to the patients.

1. Introduction

Micro-electro-mechanical-system (MEMS) technology has been successfully utilized to fabricate miniaturized devices for various applications such as optical communication, navigation and automobiles. To be further extended into biomedical applications, a MEMS-based sensor should not only precisely implement the sensing function, but also

*Corresponding author, e-mail address: g0202677@nus.edu.sg

possess excellent biocompatibility with an *in vivo* environment. This paper presents some initial results on the development of a miniature pressure sensor with a biocompatible interface. The sensor is mainly developed for therapy of temporomandibular disorder (TMD), however, other potential applications may exist as well.

TMD refers to many problems that involve the jaw muscles and temporomandibular joint. The symptoms of TMD include jaw pain, headache, jaw noise, difficulty in opening and closing the jaw, and chewing and biting difficulty. Although most people with TMD do not require medical treatment, some may develop severe complications that they have to undergo special physical therapy, orthopedic appliance therapy or even surgery. The habit of grinding and clenching the jaws, namely bruxism, is the main cause of TMD.

Bruxism may occur at any time and usually people are not aware of its occurrence. Therefore, an instrument capable of continuously monitoring the grinding activity of teeth may help patients to restrain the grinding, and thus to alleviate TMD. Using different technologies, a few devices have been developed to measure the magnitude of occlusion, and only minor modification is required to allow the monitoring of tooth-grinding activities. Among these devices, strain gauges[(1)] and quartz force transducers[(2)] make use of material deformation to measure the occlusal force, while other devices relate the bite force to the electrical activity of masticatory muscles (i.e., electromyograms or EMG).[(3)] The major drawback of these devices is their bulky size, which makes the patients uncomfortable and disturbs their everyday life. A simpler way of dealing with this problem is to use a film developed by Fuji Film of Japan, which consists of a layer of microencapsulated color-forming material and a layer of color-developing material. When pressure is applied, the microcapsules are broken and the color-forming material reacts with the color-developing material, and thus red patches appear on the film. The color density changes according to pressure level.[(4,5)] However, this film cannot be used repetitively, and hence is not suitable for continuous monitoring of the grinding of teeth.

Considering the disadvantages of above devices, a MEMS-based pressure sensor is clearly a better option for continuous monitoring of the grinding activities of the TMD patients. Owing to its small size, the microsensor, together with other ancillary miniature devices, can be embedded into a splint that is frequently encountered in orthodontics. In this paper, the sensor unit is designed, fabricated and tested. Several pressure sensing structures are investigated, including a doubly supported bridge, modified bridge with etching hole array, and four-end supported cross structures. PMMA and silicone rubber are selected as interface materials between the tooth and sensor, as these two materials have been successfully used in dentistry.

2. Design, Fabrication and Testing Methodology

2.1 *Pressure-sensing structures and design methodology*

Pressure-sensing function can be implemented by taking advantage of various physical properties of materials, including piezoelectricity, capacitance, piezoresistivity and resonance. In this work, a capacitive pressure-sensing scheme was employed because of its low power consumption, high sensitivity and existence of mature capacitive readout

method. Like a parallel-plate capacitor, the sensor consists of fixed bottom plates and flexible top plates, the latter of which are made using one of the three structures shown in Fig. 1. In comparison with membranes that are commonly used for pressure sensors, the suspended bridge structure indicated in Fig. 1(a) was believed to produce lower stress at corners, hence enabling a larger deflection and operation range. Moreover, with such a structural design, the use of a complicated reaction-sealing process that is frequently required in surface micromachined membranes could be avoided. Between neighbouring bridge units there existed etching channels that allowed the etchant to flow through and release the bridge structures. On the other hand, a modified bridge structure is also presented in Fig. 1(b), which utilizes etching holes instead of an etching channel for structure release. The region between the two dashed lines is regarded as one capacitive unit and is taken for simulation and capacitance calculation. In addition, a cross structure with four ends fixed was also investigated. The schematic of this structure is shown in Fig. 1(c).

Structural design was completed with the finite-element analysis software ABAQUS[6] for stress/deformation calculation, and with another software PATRAN[7] for modelling and postprocessing. Maximum normal stress failure theory was used as the failure criterion during design of the flexible capacitive plates, which means that the maximum principal stress induced in the structural units as shown in Fig. 1 must be lower than the fracture strength of poly-Si (1.2 GPa). The deformed structure model was extracted with PATRAN, and was then imported into the MEMS-specific simulator IntelliSuite[8] for capacitance calculation. Therefore, the correlation between the compressive loading and the capacitive response could be obtained for a single capacitive unit, which can be in turn multiplied by the capacitive unit number to obtain the capacitance response of the whole sensor. The maximum compressive load was assumed to be 5 MPa, since the maximum occlusal force and the effective contact area for a pair of molars are approximately 180 N and 6×6 mm^2, respectively. Table 1 lists the mechanical properties[9–11] used in the simulation.

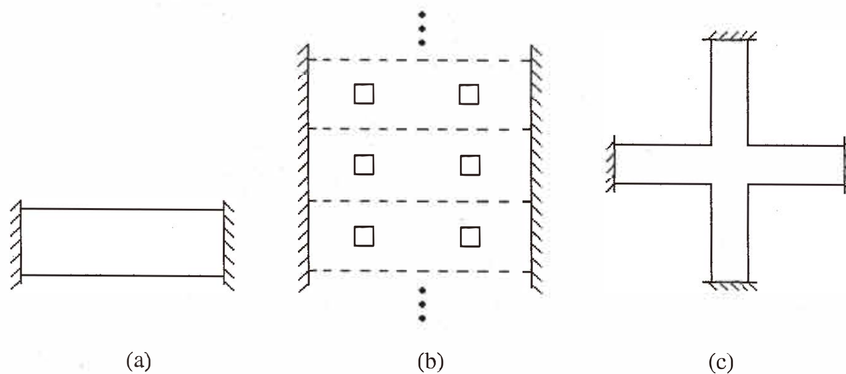

Fig. 1. Schematic of pressure-sensing structures, (a) bridge; (b) bridge with etching holes; (c) cross.

Table 1
Parameters of key layers of MUMPs process.

Film layers	Poly 1	PMMA	Silicone Rubber
Thickness, μm	2	600	600
Young's modulus, GPa	170[10]	2.38[11]	2.08E-3[11]
Poisson's ratio	0.22[10]	0.25[12]	0.48
Residual stress, MPa	–10	N/A	N/A

2.2 *Fabrication process*

Multi-user MEMS processes (MUMPs) by Cronos Integrated Microsystems is a commercial program that provides the international industry and academic communities with surface micromachining technology. This process includes deposition and patterning of one silicon nitride layer, three poly-Si layers, two silicon oxide layers and one metallization layer.[12] In this work, a poly 1 layer produced by MUMPs was employed to form the top flexible capacitive plate, and the poly 0 layer was used as the bottom fixed capacitive plates. The silicon oxide layer between these two poly-Si layers is etched away in a 49% HF solution and hence the top capacitive plate became flexible.

2.3 *Measurement methods*

Initial testing was conducted to investigate the capacitance response of fabricated sensors upon the application of external load. As shown in Fig. 2, a PMMA or silicon rubber slice of 0.6 mm thick was glued on top of the sensor chips and a Kapton film from Dupont with excellent dielectric properties was introduced between the silicon chip and steel anvil. Compressive load was applied with an Instron Microtester 5848 to perform a basic exploration of the viability of these sensors. An XE2004 chip from XEMICS of Switzerland, which converts a capacitance difference input into a voltage output, was used to obtain the capacitance response of the pressure sensors upon external loading. The procedure is as follows. First, to guarantee that the XE2004 operated in its effective range, a regulating capacitor was connected in series with the capacitive sensor to form a variable capacitor. A reference capacitor of 47 pF was used and the power supply to the XE2004 chip was set to 3.0 V. Under these conditions, the XE2004 chip was calibrated and the correlation between the voltage output V (in volts) and the variable capacitance C_1 (in pF) was obtained as

$$V = 0.733 - 0.015 \times C_1 . \tag{1}$$

On the basis of this equation, the capacitance response of the pressure sensor under compressive loadings can be inversely deduced from the measured voltage, and thus the correlation between loading magnitude and sensor capacitance could be obtained.

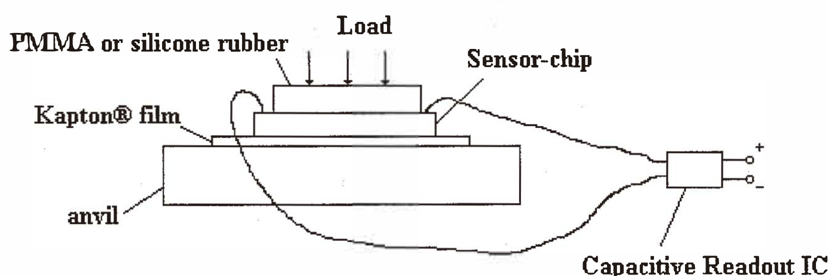

Fig. 2. Testing setup for fabricated sensor chips.

3. Results and Discussion

3.1 *Structural design*

As mentioned previously, simulation was conducted for structural design and optimization of the top flexible capacitive plates. For all these three structures, it should be noted that, according to the design rules of MUMPs, the distance between two neighbouring etching channels or holes must be less than 25 μm for best releasing results. Therefore, the width of bridge beams is set to 25 μm, while the nominal width (i. e., the distance between two dash lines) of modified bridges is set to 30 μm with etching holes of 5x5 μm^2. For the cross structure, the width of crossing bridges were reduced to 20 μm to ensure the central part of the cross structure was fully released.

Figure 3 shows simulation results of three structures covered by either silicone rubber or PMMA. At a certain compressive loading level such as 5 MPa, both the deflection and the induced maximum principal stress increase with the beam width. Based on these results, the beam lengths of three different structures were determined as shown in Table 2. It was noticed that, for the modified bridge structure, the etching holes could be arranged along the beam length in two ways. First, the distance between etching holes was maintained at 25 μm, which is the maximum distance required by the fabrication process for best releasing results. Second, the etching holes were evenly distributed along the beam length, thus the distance between etching holes depended on the beam length. It was observed that the beam deflection was almost the same for both types of etching hole distribution, while the maximum principal stress of beams with etching holes separated by a fixed distance of 25 μm was much lower than that of beams with etching holes uniformly distributed, as shown in Fig. 3(b). Clearly, a higher deflection and thus higher capacitance change could be obtained by beams with etching holes separated by 25 μm.

It could be observed from Table 2 that the two bridge structures have quite similar deformation behaviors. Simulation also suggested that the maximum principal stress exists at the central region of these two bridge structures. Since a larger capacitive plate area could be obtained with the modified bridge structure, however, it was expected that the capacitance response would be larger than that of the simple bridge structure. On the

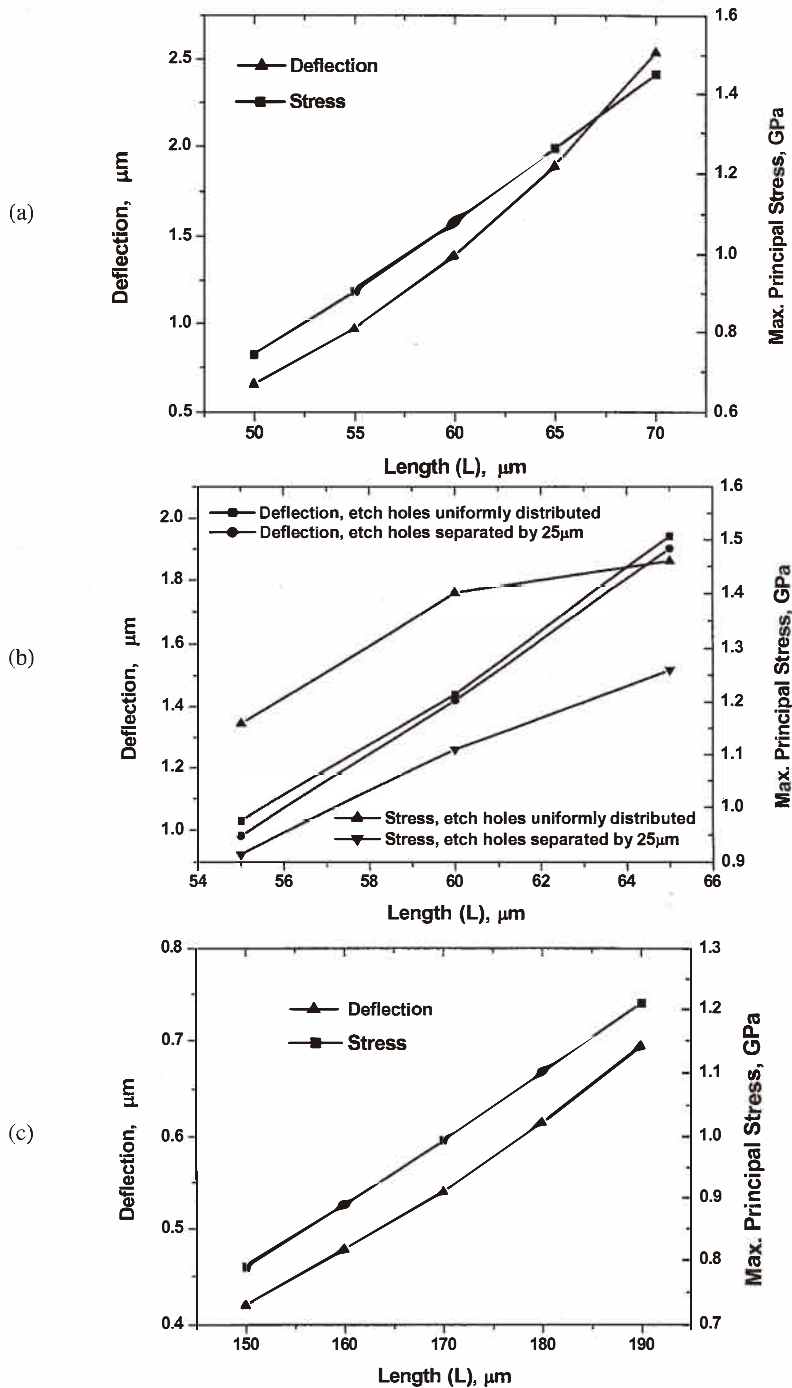

Fig. 3. Deflection and maximum principal stress of pressure-sensing structures at P=5 MPa, (a) bridge with silicone rubber; (b) bridge with silicone rubber and etching holes; (c) cross with PMMA.

Table 2
Dimensions and deformation of pressure-sensing structures.

Structure	Length μm	Width μm	Distance between holes, μm	Deflection μm	Stress GPa
Bridge/silicon rubber	60	25	N/A	1.39	1.08
Modified bridge/silicon rubber	60	30	25	1.4	1.11
Cross/PMMA	170	20	N/A	0.54	0.99

other hand, a much lower deflection was observed on the cross structure, implying that its operation range would be smaller than the bridge structures. The maximum principal stress was observed at the four intersecting corners of the cross structure, where stress concentration was expected to occur. Figure 4 showed photographs of three pressure-sensing structures fabricated with dimensions as shown in Table 2. From Fig. 4, it could also be observed that the cross structure utilized the design area less effectively than the bridge structures.

3.2 *Capacitance calculation*

For the methods described in section 2.1, the capacitance response of the three pressure sensing structures is shown in Fig. 5. It should be noted that only one single structural unit is taken for calculation here. As shown in the figure, the capacitance of both bridge structures gradually deviated from the linear range with increasing pressure, while the capacitance of the cross structure increases linearly with pressure due to its small deflection. Considering that, under compressive loading, the capacitive response of a single sensor unit was too small to be detected. The whole sensor was composed of a large number of capacitive units connected in parallel. Since a chip area of approximately 4.5×3 mm^2 was assumed for all of the three designs, the capacitive unit number in a sensor chip and the corresponding sensor sensitivities were calculated and are summarized in Table 3. It could be observed that the modified bridge sensor demonstrated higher capacitive response than the bridge sensor, and the sensor with cross structures has the lowest sensitivity due to the small deflection of beams.

3.3 *Testing*

With the method introduced in section 2.3, the capacitance response of sensors with either silicone rubber or PMMA as an interface was related to the external compressive loading. It could be observed that for both bridge and modified bridge structure sensors, the capacitance remained almost the same during the low force range, while capacitance kept changing with load in the case of a cross structure sensor. Considering the difference in stiffness of silicone rubber and PMMA, it was evident that silicone rubber may deform more easily to accommodate the load exerted on it, and thus the capacitance response of the sensor might not be observed in a low force range. For all of these three sensor designs, a quasi-linear correlation between capacitance and the compressive loading was observed in

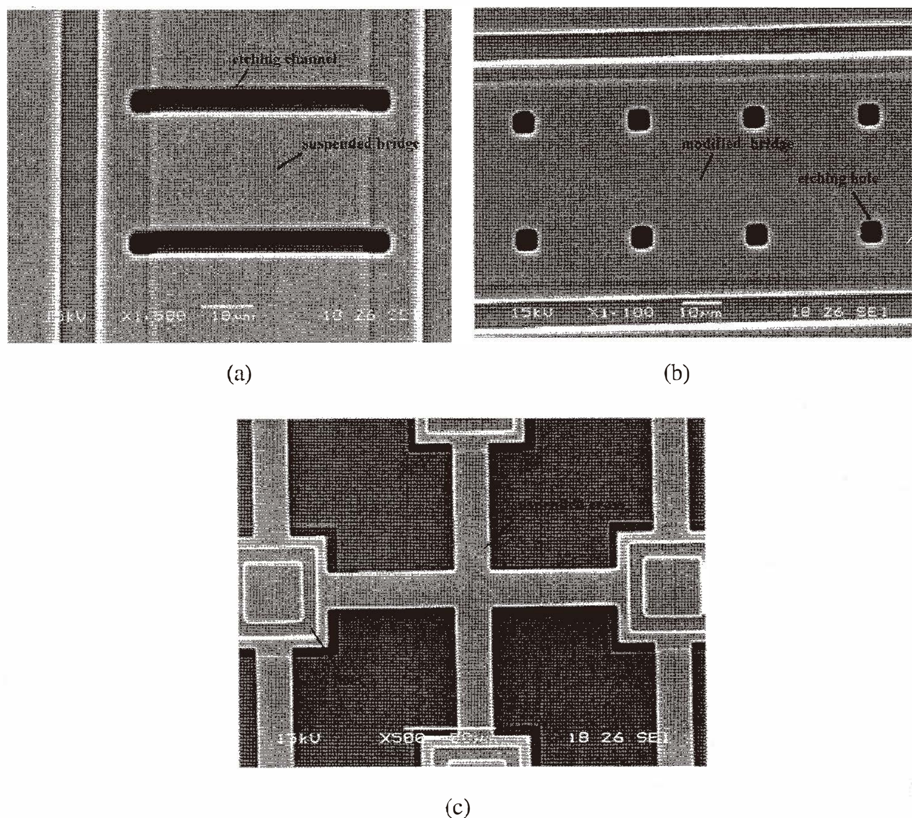

Fig. 4. Photographs of pressure-sensing structures. (a) bridge; (b) modified bridge; (c) cross.

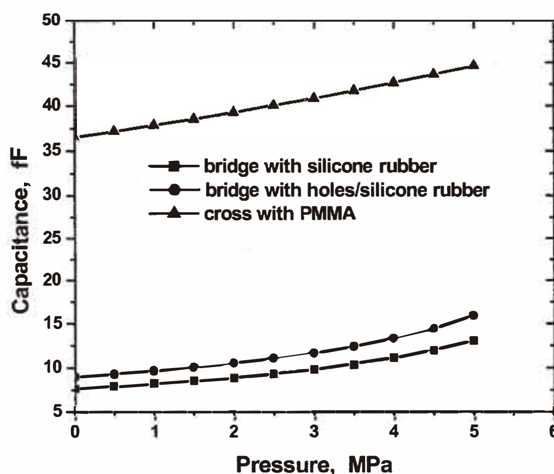

Fig. 5. Calculated capacitance response of single structural units.

Table 3
Geometric parameters and sensitivities of pptimised pressure sensors.

Strucutre	Area per unit (μm^2)	No. of units	Sensitivity at P=5 MPa (pFM/Pa)
Bridge/silicone rubber	60×25	38×38	3.43
Modified bridge/silicon rubber	60×30	37×82	4.21
Cross/PMMA	170×170	18×20	0.58

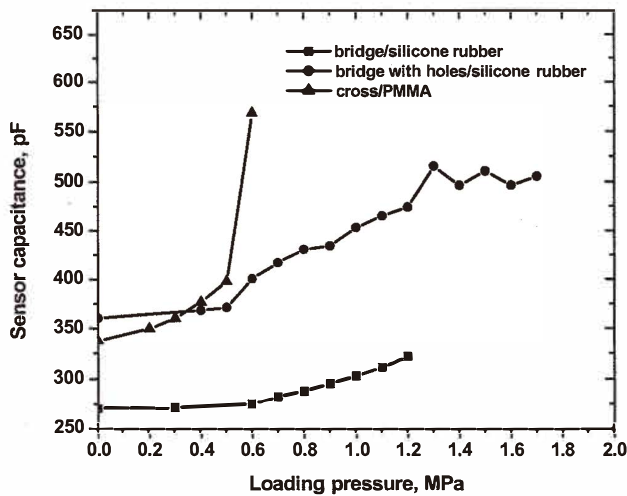

Fig. 6. Sensor capacitance response upon loading pressure.

a certain pressure range. This may be regarded as the effective working regime of the sensors. During this quasi-linear range, the sensitivities of the bridge, modified bridge and cross structure sensors were measured to be 77.1 pF/MPa, 111.6 pF/MPa and 120.1 pF/MPa, respectively.

A significant difference existed between the calculated and measured capacitance values of the sensors. For example, the static capacitances of the cross sensor were 13.14 pF and 337.61 pF by calculation and measurement, respectively. Some factors may contribute to this difference. First, incomplete etching of SiO_2 during sensor fabrication may result in a higher capacitance due to its higher dielectric constant (~3.9). The presence of remanent silicon dioxide was verified by a nano-indentation test as shown in Fig. 7. Significant discontinuities were observed in the loading sections of force-deflection curves for both bridge and modified structures, implying that some oxide survived the etching process but were crashed during the application of compressive loading. In addition, the presence of remanent oxide was also revealed by the indentation curve of the cross

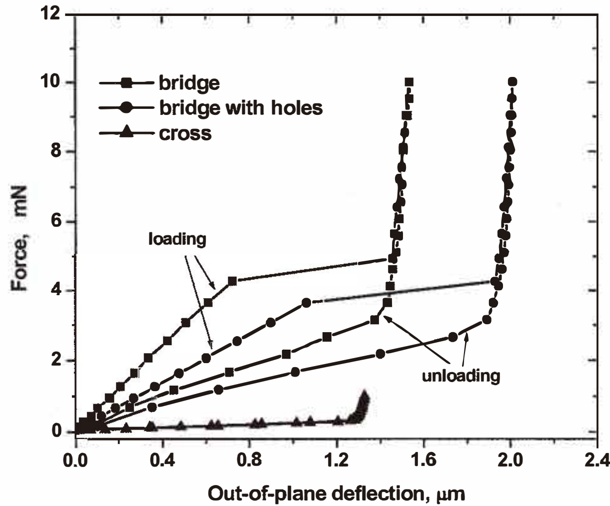

Fig. 7. Deflection of structural units by nano-indentation.

structure, from which a maximum deflection of approximately 1.3 μm, markedly less than the nominal oxide thickness (2 μm) presumed by MUMPs, was observed. Second, during simulation an even pressure was assumed on the silicone rubber or PMMA, but in measurement a nonuniform pressure distribution may exist due to the existence of the posts supporting the pressure sensing structures. This difference may become more significant within the higher range of compressive loading. Finally, the PCB, wires connecting sensors with capacitive readout IC and other testing setup components were all potential sources of parasitic capacitance. Efforts are being made to improve the silicon oxide etching process and *in vivo* testing will be conducted to verify its practical application.

4. Conclusions

With either silicone rubber or PMMA as the interface, three pressure sensing structures, including bridge, modified bridge with holes, and cross structure, were designed and fabricated by surface micromachining technology. An nonuniform distribution of holes in the modified bridge structure was found to produce less stress and hence a larger operation range. Although a significant difference exists between calculation and measurement, initial testing results proved the viability of these sensors for therapy of TMD. Compared with conventional methods, the micromachined sensor enables continuous monitoring of tooth-grinding activities and is less injurious to the patients.

Reference

1 D. J. Anderson: Journal of Dental Research **35** (1955) 664.
2 A. Waltimo and M. Kononen: Scandinavian Journal of Dental Research **101** (1993) 171.
3 Y. Kawazoe: Journal of Dental Research **58** (1979) 1440.
4 O. Hidaka, M. Iwasaki, M. Saito, and T. Morimoto: Journal of Dental Research **78** (1999) 1336.
5 H. Kurita, K. Ikeda, K. Kurashina: Journal of Oral Rehabilitation **27** (2000) 79.
6 ABAQUS V5.8, Hibbitt, Karlsson & Sorensen, Inc. 1080 Main Street Pawtucket, Rhode Island 02860-4847, USA.
7 PATRAN, MSC Software Corporation, 2 MacArthur Place, Santa Ana, CA 92707, USA.
8 IntelliSuite, Intellisense Corporation, 36 Jonspin Rd., Wilmington, MA 01887, USA.
9 W. N. Sharpe, Jr., B. Yuan and R. L. Edwards: Journal of Microelectromechanical Systems **6** (1997) 193.
10 Biomaterials Properties Database, University of Michigan. URL: http://www.lib.umich.edu/dentlib.html
11 R. S. Lakes: Viscoelastic Solids, published by CRC Press, 1999, pp 247.
12 Cronos/MUMPs Design Rule, V6.0. Cronos Integrated Microsystem Inc., 3026 Cornwallis Road, Research Triangle Park, NC 27709, USA.